Supplement of Atmos. Chem. Phys., 18, 385–403, 2018
https://doi.org/10.5194/acp-18-385-2018-supplement

Atmospheric Chemistry and Physics
Open Access
EGU

Supplement of

Highly controlled, reproducible measurements of aerosol emissions from combustion of a common African biofuel source

Sophie L. Haslett et al.

Correspondence to: Hugh Coe (hugh.coe@manchester.ac.uk)

S1 Fragmentation table updates for AMS analysis

Description for table S1.

The fragmentation table for AMS data has been developed to quantify the proportion of each *m/z* peak that can be attributed to each species measured by the AMS (organics, NO3 etc.; Allan et al. 2004). This was established using typical mass spectra from ambient measurements. During biomass burning, however, the contribution of sulphate to the overall mass spectrum is considerably lower. Typically, sulphate loadings are calculated first and organics are treated as an interference on the sulphate peaks. Ortega et al. (2013) suggest a modification to the fragmentation table in which sulphate is instead treated as an interference on the organic peaks, given that organics are so much more dominant in pure biomass burning emission. The same adjustments to the fragmentation table were made as those shown by Ortega et al. (2013) in their table S1.

Further adjustments were made to the fragmentation table to account for the dilution of the emissions in nitrogen before being measured by the AMS. All air peaks that are based on the nitrogen peak at *m/z* 28 were updated as shown in table S1 here.

Table S1: Fragmentation table updates for unit mass resolution AMS analysis due to nitrogen dilution.

Fragment	Standard entry	Updated entry
CO2[44]	0.00037*1.36*1.28*1.14*frag_air[28]	0.01*0.00037*1.36*1.28*1.14*frag_air[28]
RH[18]	0.01*frag_air[28]	0.001*frag_air[28]
O16[16]	0.353*frag_air[14]	0.01*0.353*frag_air[14]
air[40]	0.009*1.11*1.28*1.14*frag_air[28]	0.01*0.009*1.11*1.28*1.14*frag_air[28]

S2 Time series for each experiment carried out

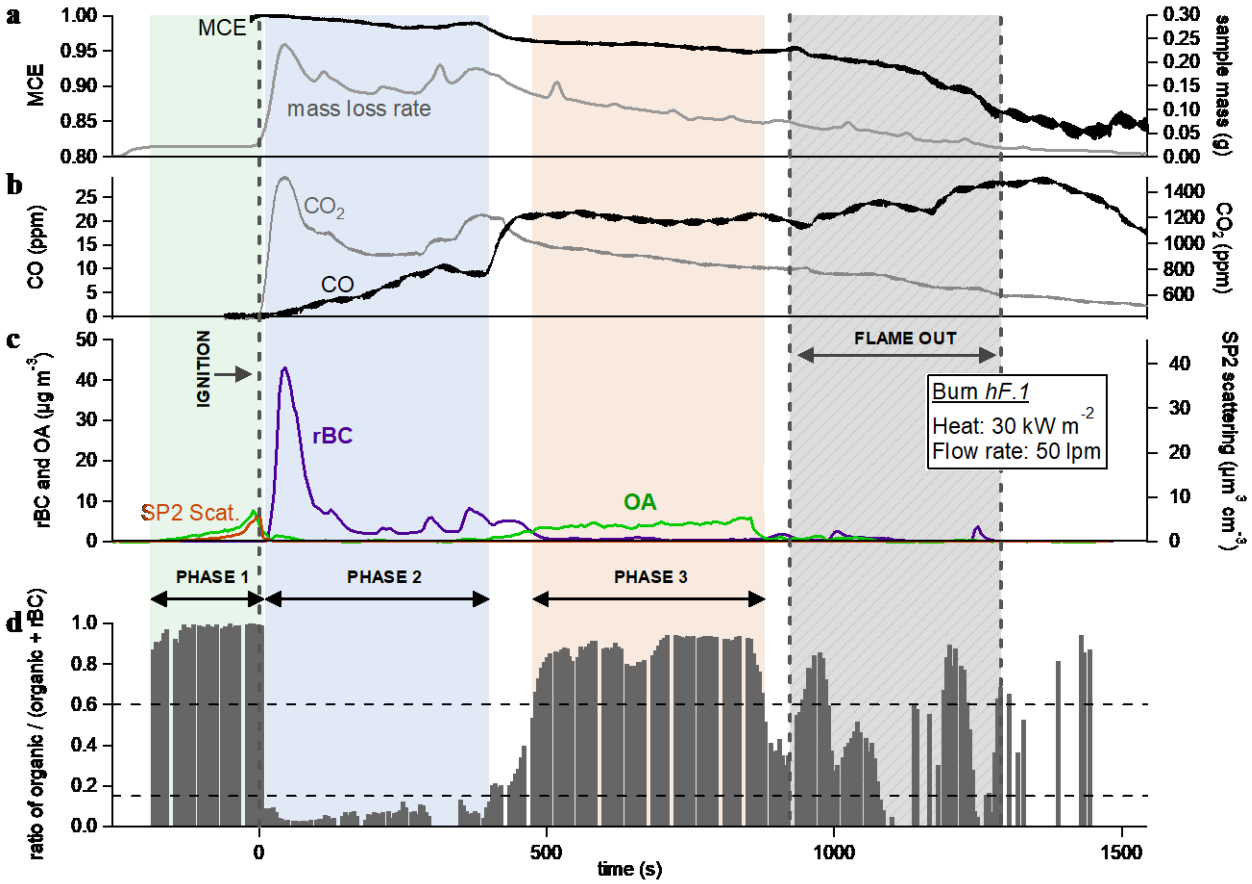

Figure S1.1: time series for experiment *hF.1*

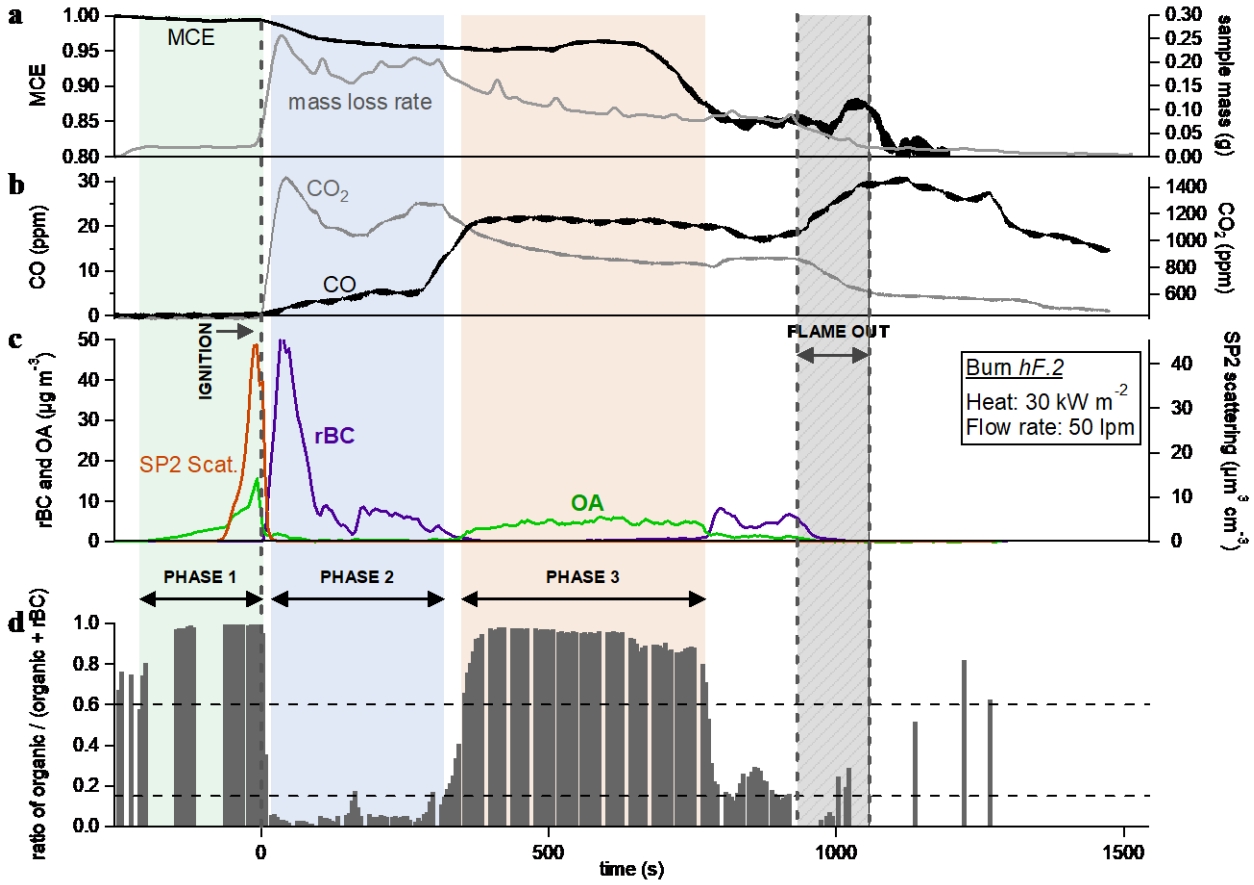

Figure S1.2: time series for experiment *hF.2*

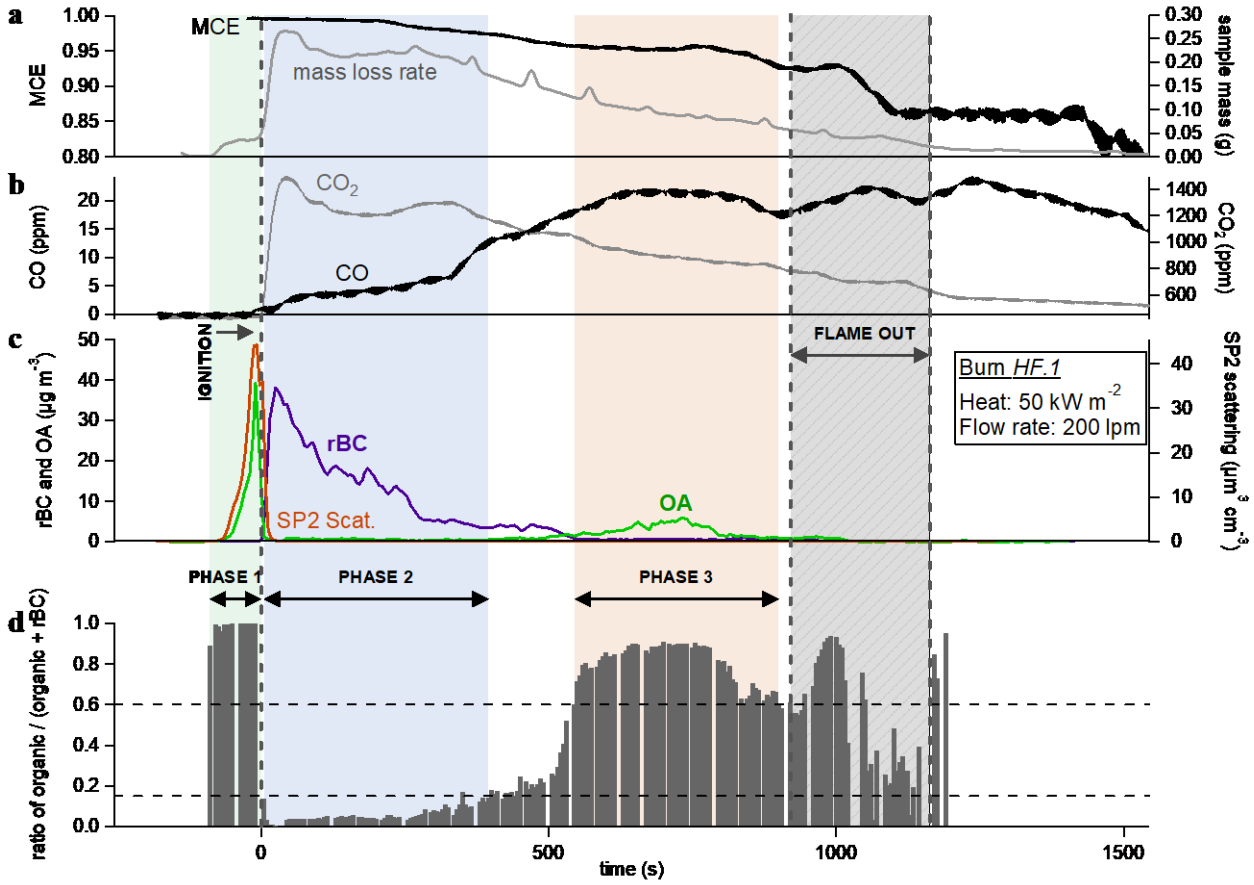

Figure S1.3: time series for experiment *HF.1*

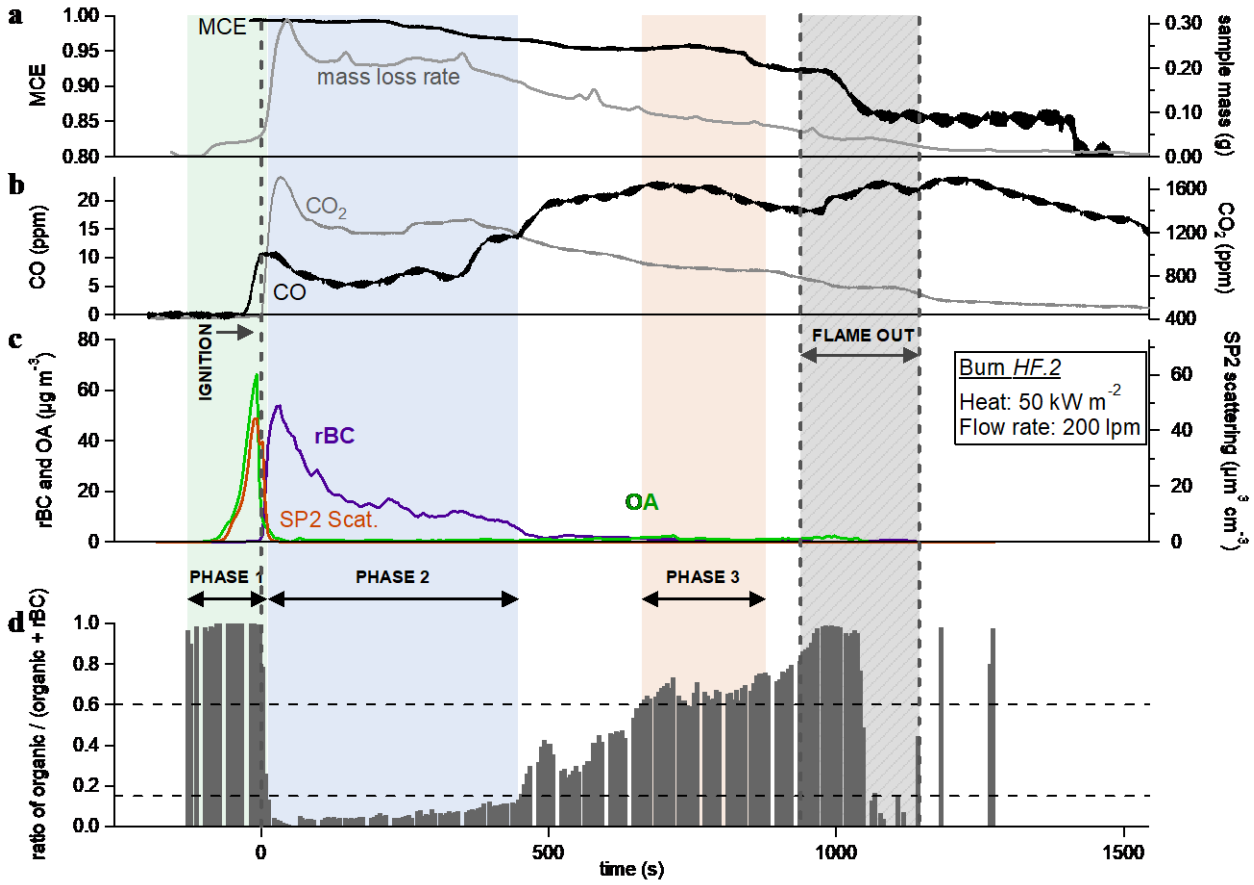

Figure S1.4: time series for experiment *HF.2*

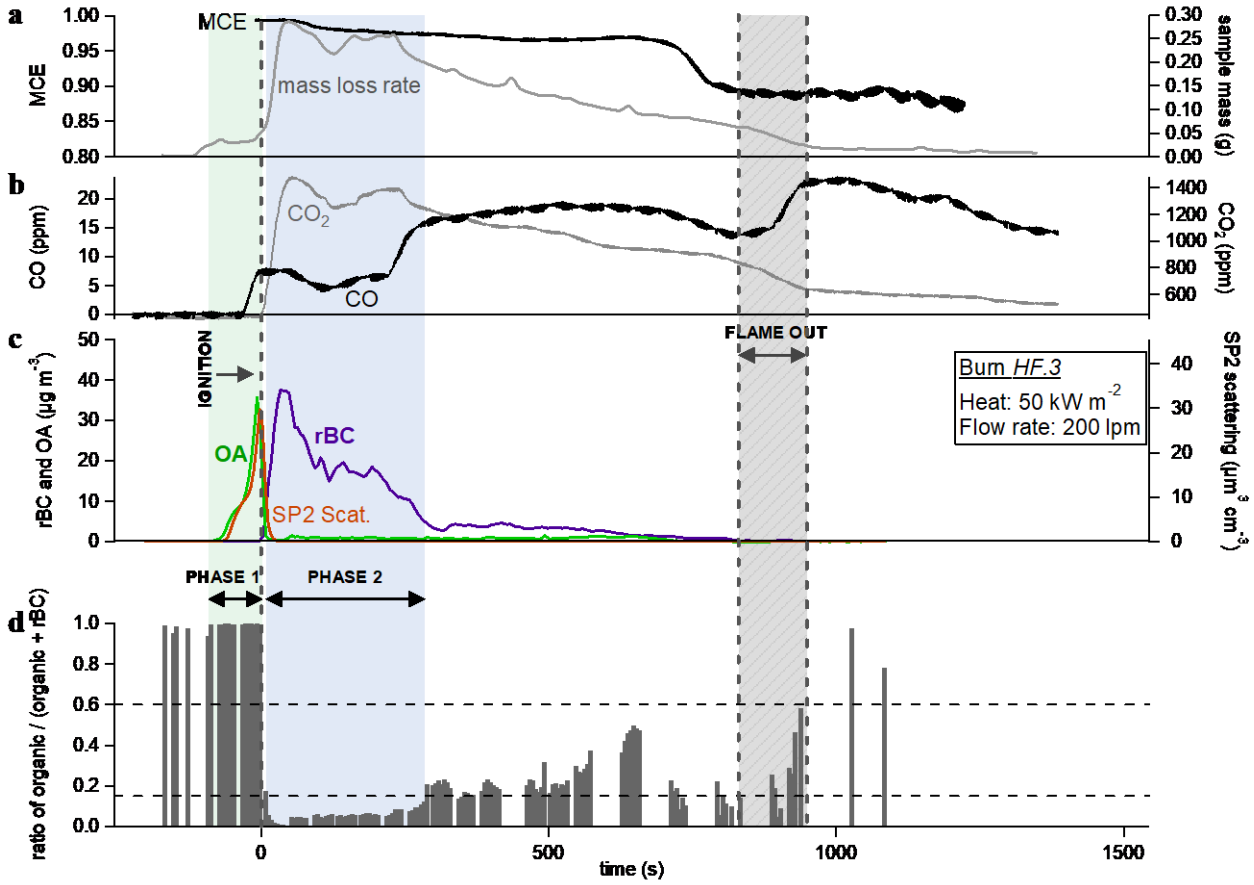

Figure S1.5: time series for experiment *HF.3*

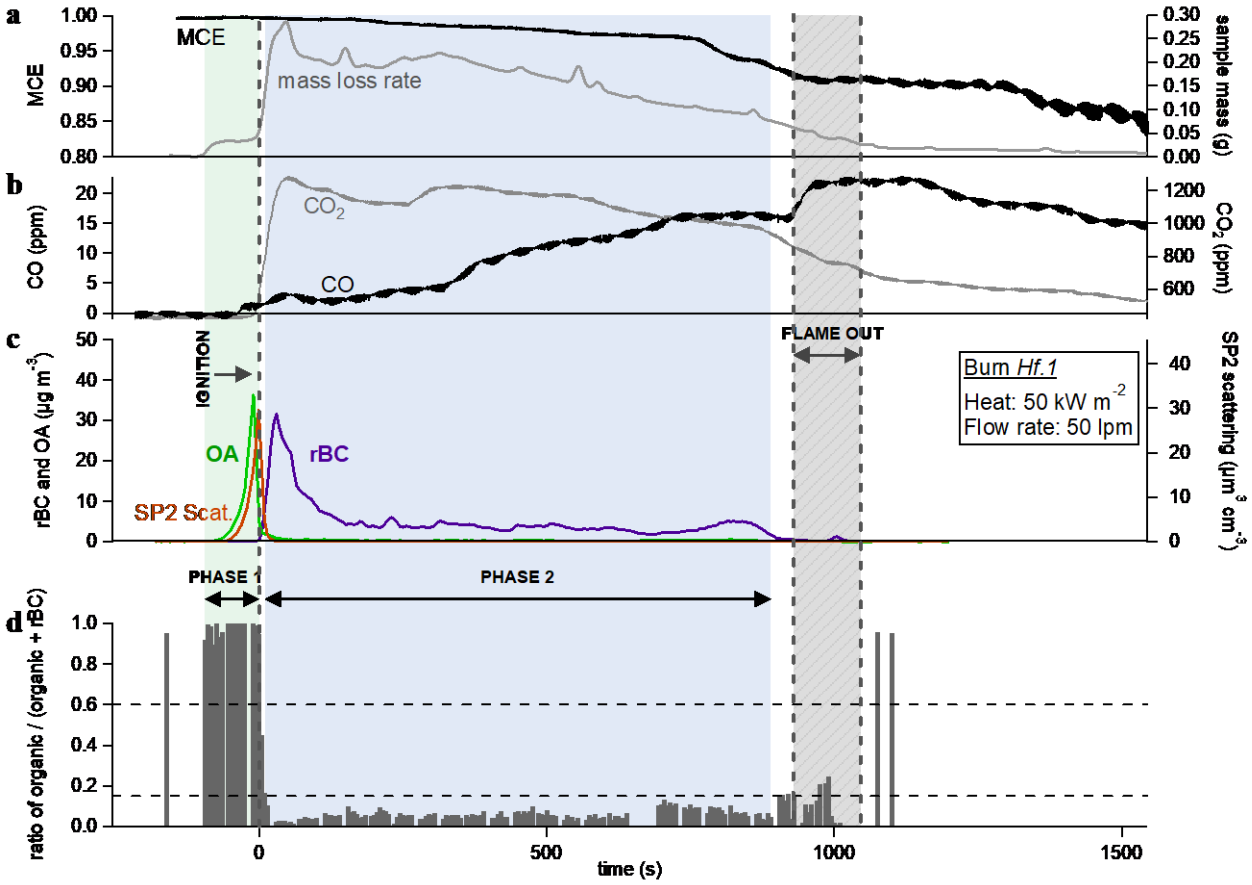

Figure S1.6: time series for experiment *Hf.1*

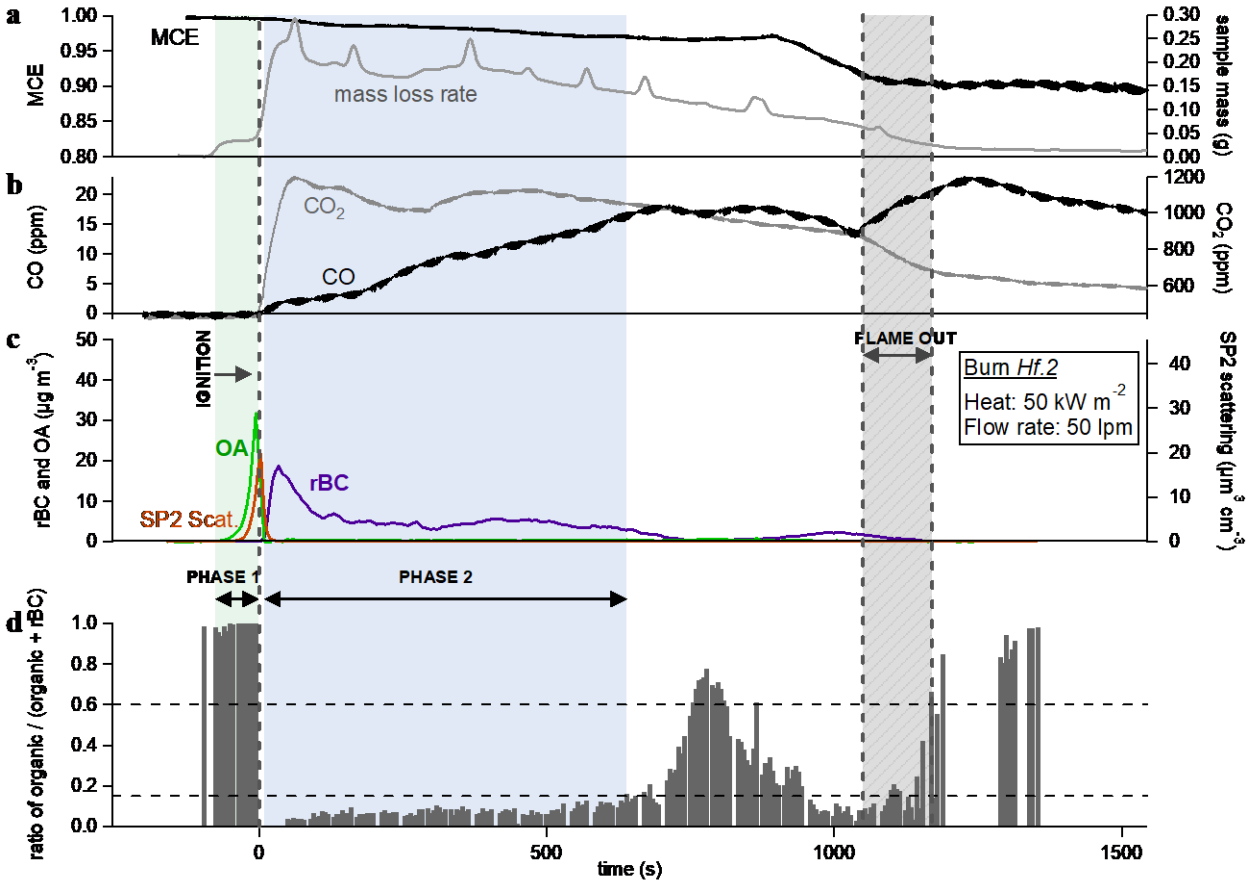

Figure S1.7: time series for experiment *Hf.2*

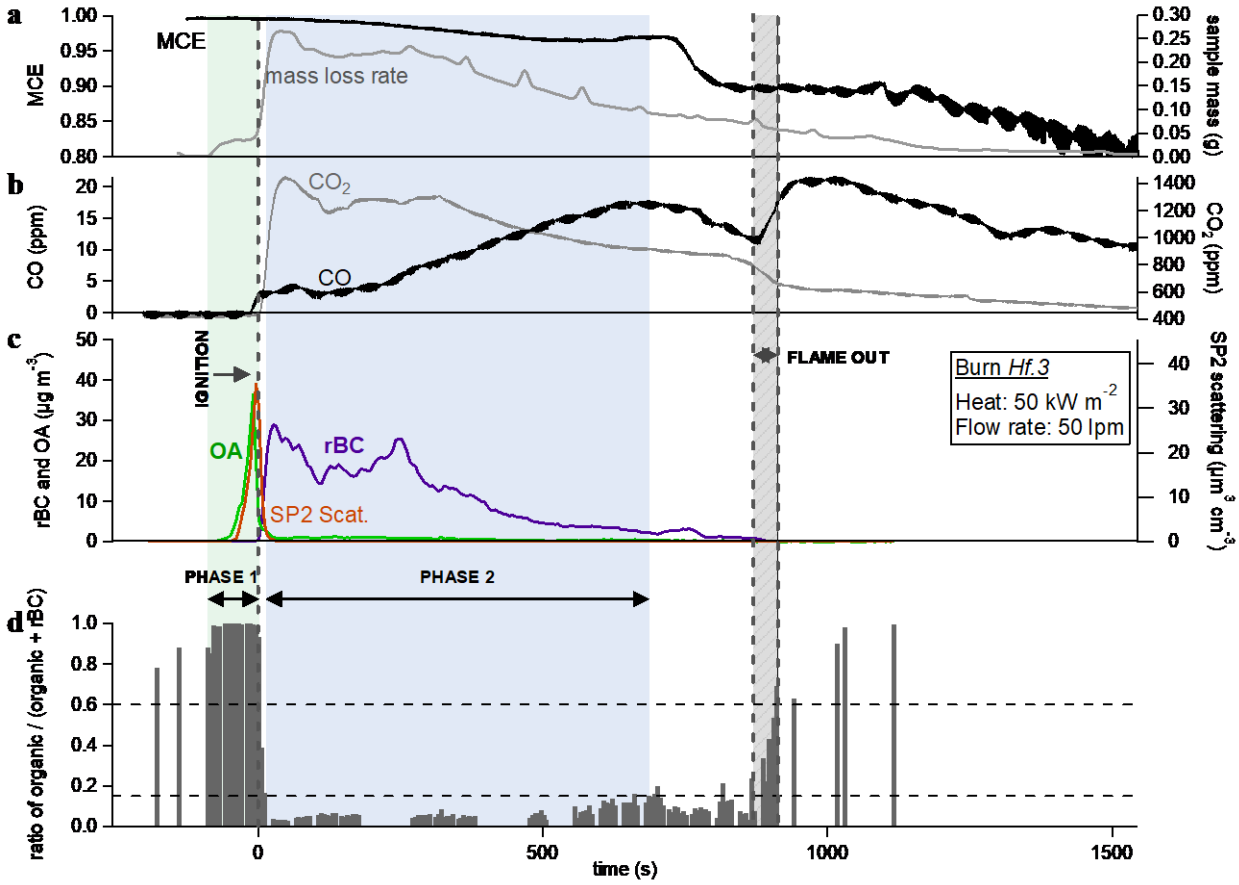

Figure S1.8: time series for experiment *Hf.3*

S3 OA and rBC concentrations vs mass loss for each experiment carried out, averaged over 5 s.

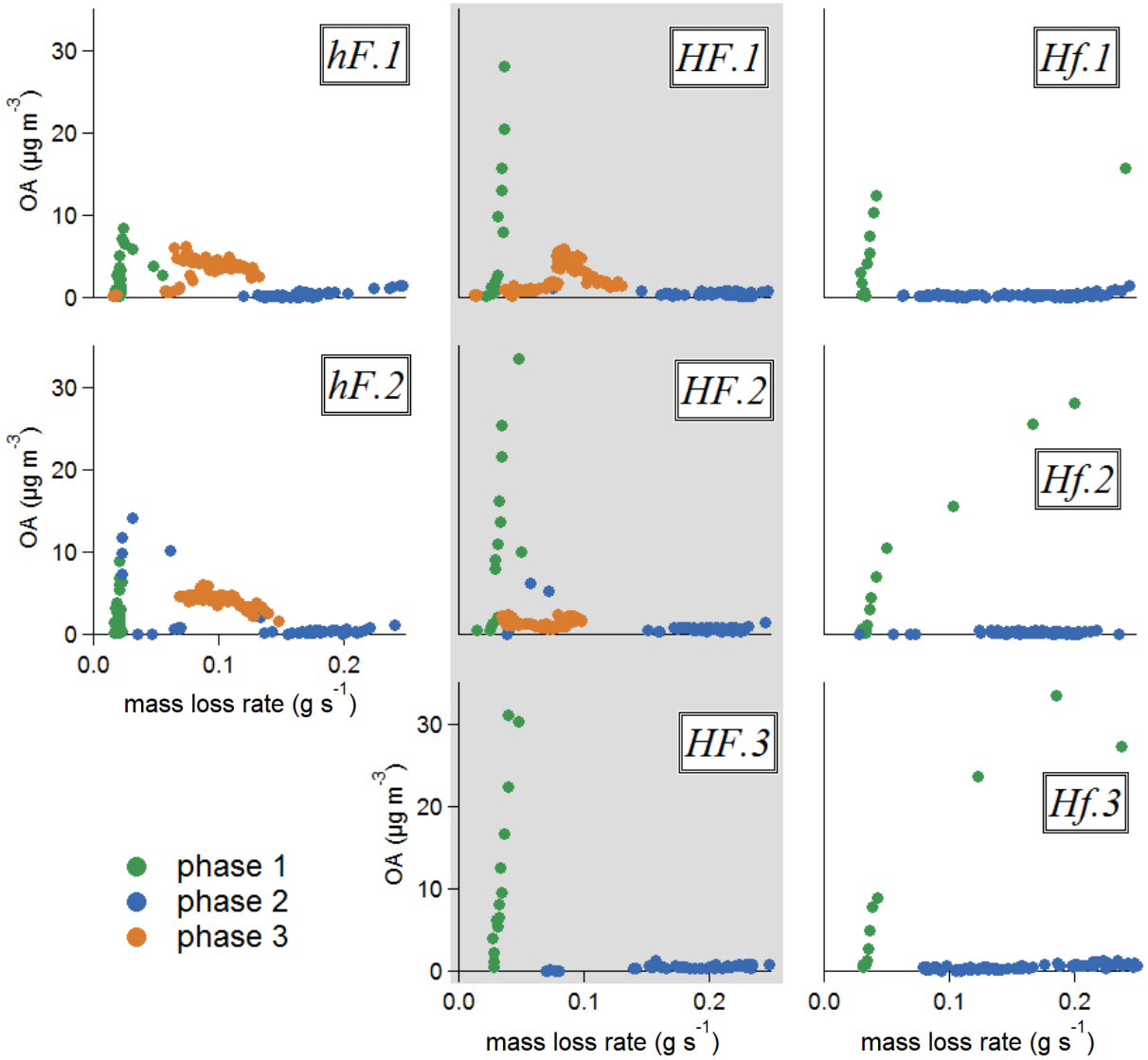

Figure S2: OA emissions vs mass loss for each experiment, averaged over every 5 seconds.

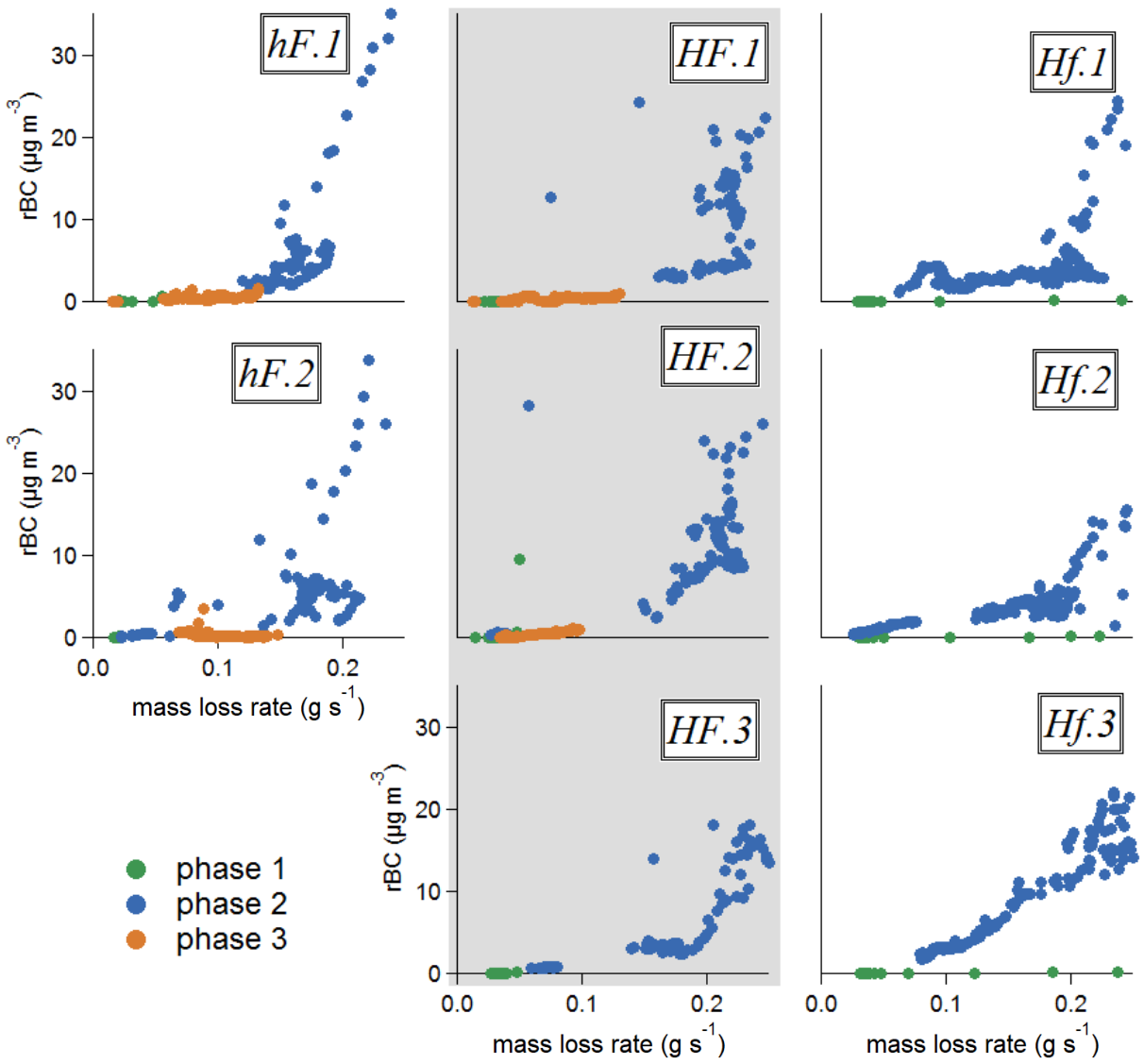

Figure S3: rBC emissions vs mass loss for each experiment, averaged over every 5 seconds.

S4 Alkali metal measurements

During the flaming period of each test (phase 2), extremely large quantities of potassium were recorded by the AMS at *m/z* 39 and 41; at times, enough to saturate the instrument. Such measurements are routinely discarded, as the thermal ionisation of alkali metals on the AMS heater result in large, unquantitative measurements. However, qualitatively, measurements of potassium were high during phase 2. Large peaks at *m/z* 85 and 87 were consistent with the naturally-occurring isotope ratio of rubidium-85 to rubidium-87, suggesting that alkali metals in general were emitted during this phase. The natural and measured abundances of these species are shown in table S1.

Table S1: Natural and measured abundances of alkali metals.

Isotopes	Natural abundance	Measured abundance
Potassium K-39 : K-41	0.932 : 0.067	0.934 : 0.066
Rubidium Rb-85 : Rb-87	0.722 : 0.278	0.713 : 0.287